

# Comparison between Simulation and Experiment on Injection Beam Loss and Other Beam Behaviours in the SPring-8 Storage Ring

Presented by Hitoshi TANAKA,

Contributors: Jun SCHIMIZU,  
Kouichi SOUTOME, Masaru TAKAO

JASRI/SPring-8

# Contents

1. Motivation
2. Simulation Model
3. Comparison between Simulation and Experiments
4. Summary
5. Tentative FMA Results

# 1. Motivation

- In ideal top-up operation, **reduction of injection beam loss** and suppression of stored beam oscillation by frequent beam injections are **critically important**.

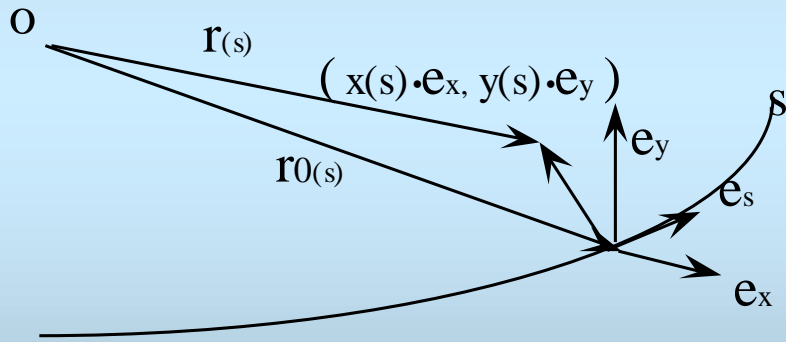
- Aiming at understanding of mechanism of injection beam loss and its suppression, a precise simulation model has been developed.

**Key:** Precise simulation of particle motion with a large amplitude ( $x \sim \pm 10\text{mm}$ )

# 2. Simulation Model

## 2.1. Hamiltonian

$$H = \hat{p}_\sigma - h \cdot \left[ \left\{ (1 + \delta)^2 - (\hat{p}_x - \frac{e}{P_0} A_x)^2 - (\hat{p}_y - \frac{e}{P_0} A_y)^2 \right\}^{1/2} - \frac{e}{P_0} A_s \right], \quad (1)$$



where  $(x, \hat{p}_x \equiv \frac{p_x}{p_0})$ ,

$(y, \hat{p}_y \equiv \frac{p_y}{p_0})$ ,

$(\sigma \equiv s - v_0 t, \hat{p}_\sigma \equiv \frac{E - E_0}{p_0 v_0})$ ,  $\delta \equiv \frac{p - p_0}{p_0}$ ,

$h \equiv 1 + \frac{x}{\rho_x(s)} + \frac{y}{\rho_y(s)}$ .

Refs. [1] D.P. Barber, G. Ripken, F. Schmidt; DESY 87-036

[2] G. Ripken; DESY 87-036

## 2.2. Components and their Symplectic Integration

### (a) Bending Magnet

Equation (1) is integrated without expanding the square root part.

Analytical solutions derived by E. Forest are used for “rectangular” and “sector” magnet integration.

Ref. [3] E. Forest, M.F. Reusch, D.L. Bruhwiler, A. Amiry;  
Particle Accel.45(1994)65.

## 2.2. Component Model and Symplectic Integration (2)

### (b) Quadrupole and Sextupole Magnets

In this case, Eq. (1) has a separating form of  $A(p) + V(x)$ .

4th order explicit integration method is adopted. Sextupoles are treated as thick elements.

- Refs. [4] E. Forest and R.D. Ruth; *Physica D* 43 (1990)105.  
[5] H. Yoshida; *Celestial Mechanics and Dynamical Astronomy* 56 (1993) 27.

## 2.2. Component Model and Symplectic Integration (3)

### (c) Other Magnets (except for IDs)

All other magnetic components are treated as **thin kicks**.

Multi-pole up to 20 poles available.

### (d) RF Cavities (Ref. [1])

Cavities are treated as thin elements.

$$\frac{e}{p_0} A_s = \frac{-L}{2\pi k} \cdot \frac{e}{p_0} \cdot V(s) \cdot \left[ \cos\left(\frac{2\pi k}{L} \cdot \sigma + \varphi\right) + G \cdot \frac{2\pi k}{L} \cdot \sigma \cdot \sin \varphi \right], \quad (2)$$

$G = 1$  without Radiation,  $G = 0$  with radiation.

## 2.2. Component Model and Symplectic Integration (4)

### (e) Radiation Effects

Ref. [6] M. Sands; Report SLAC-121 (1970).

Normalized photon energy spectrum + random number ranging from 0 to 1

Radiation from BMs, QMs, SMs and IDs are considered.

### (f) Fringe Fields

Lowest order effect is only considered for BMs, QMs and SMs.

BM fringe -> 
$$H_{\pm} = \pm K_x \cdot \frac{\frac{1}{2} \cdot y^2 \cdot p_x}{\sqrt{(1+\delta)^2 - p_x^2 - p_y^2}}, \quad K_x = \frac{1}{\rho} \cdot \quad (\text{Ref. [3]}) \quad (3)$$



## 2.3. Magnetic Errors

### (a) Normal and Skew Quadrupole Errors [7]

236 Q-error kicks and 132 SQ-error kicks are considered. These strengths are estimated by fitting measured beam response with 4x4 formalism.

### (b) Multipole errors

Systematic errors lower than 20 poles are considered. 10pole for BM and 12pole for QM.

Ref. [7] J. Safranek; NIMA 388 (1997)27.

## 2.4. ID Model

$$\begin{aligned} \frac{e}{p_0} A_x &= \frac{\rho_0^{-1}}{kz} \cdot \cos(kx \cdot x) \times \cosh(ky \cdot y) \times \sin(kz \cdot z) \\ &- \hat{\rho}_0^{-1} \cdot \frac{\hat{k}y}{kz \cdot \hat{k}x} \cdot \sinh(\hat{k}x \cdot x) \times \sin(\hat{k}y \cdot y) \times \sin(kz \cdot z + \varphi) \end{aligned} \quad (4)$$

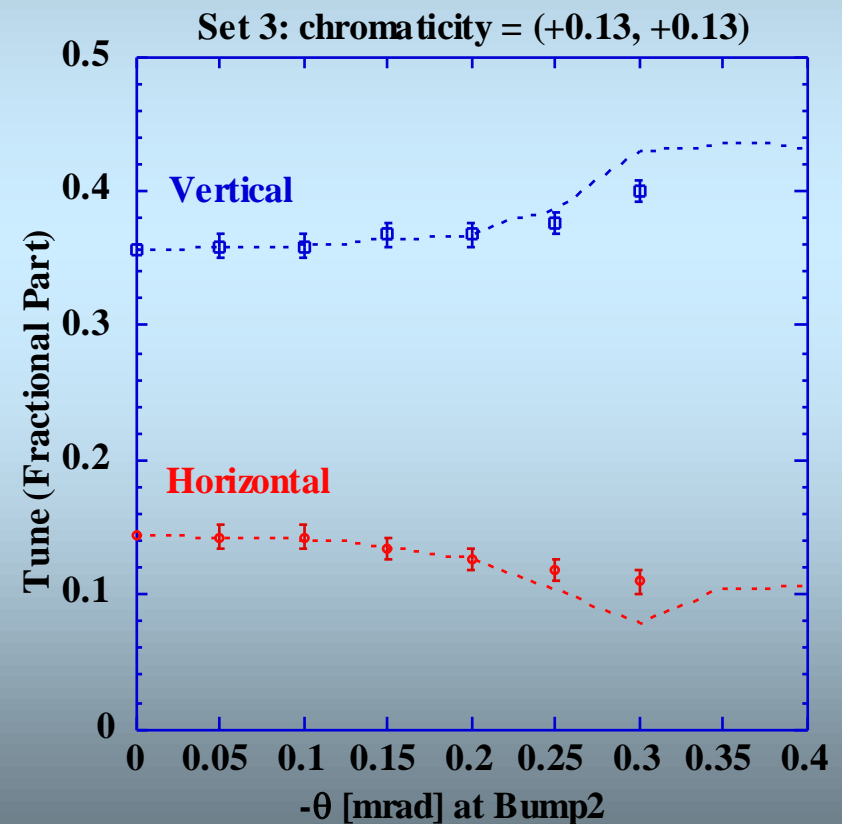
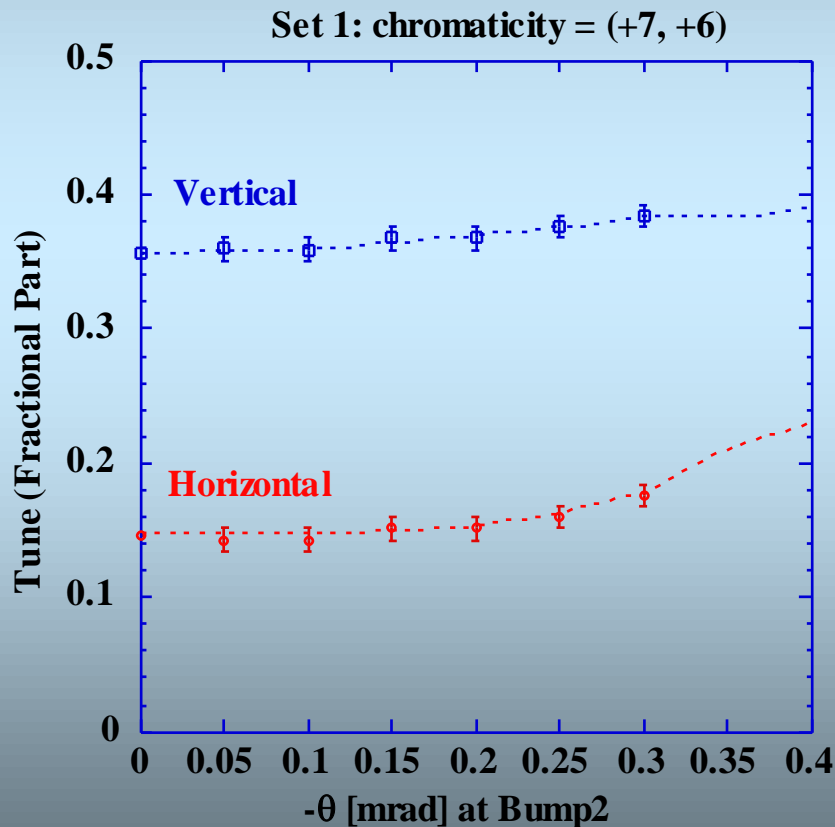
$$\begin{aligned} \frac{e}{p_0} A_y &= \rho_0^{-1} \frac{kx}{kz \cdot ky} \cdot \sin(kx \cdot x) \times \sinh(ky \cdot y) \times \sin(kz \cdot z) \\ &- \frac{\hat{\rho}_0^{-1}}{kz} \cdot \cosh(\hat{k}x \cdot x) \times \cosh(\hat{k}y \cdot y) \times \sin(kz \cdot z + \varphi) \end{aligned}$$

For ID integration, the square root of Eq.(1) is expanded and the lowest order parts are only integrated by means of a generating function.

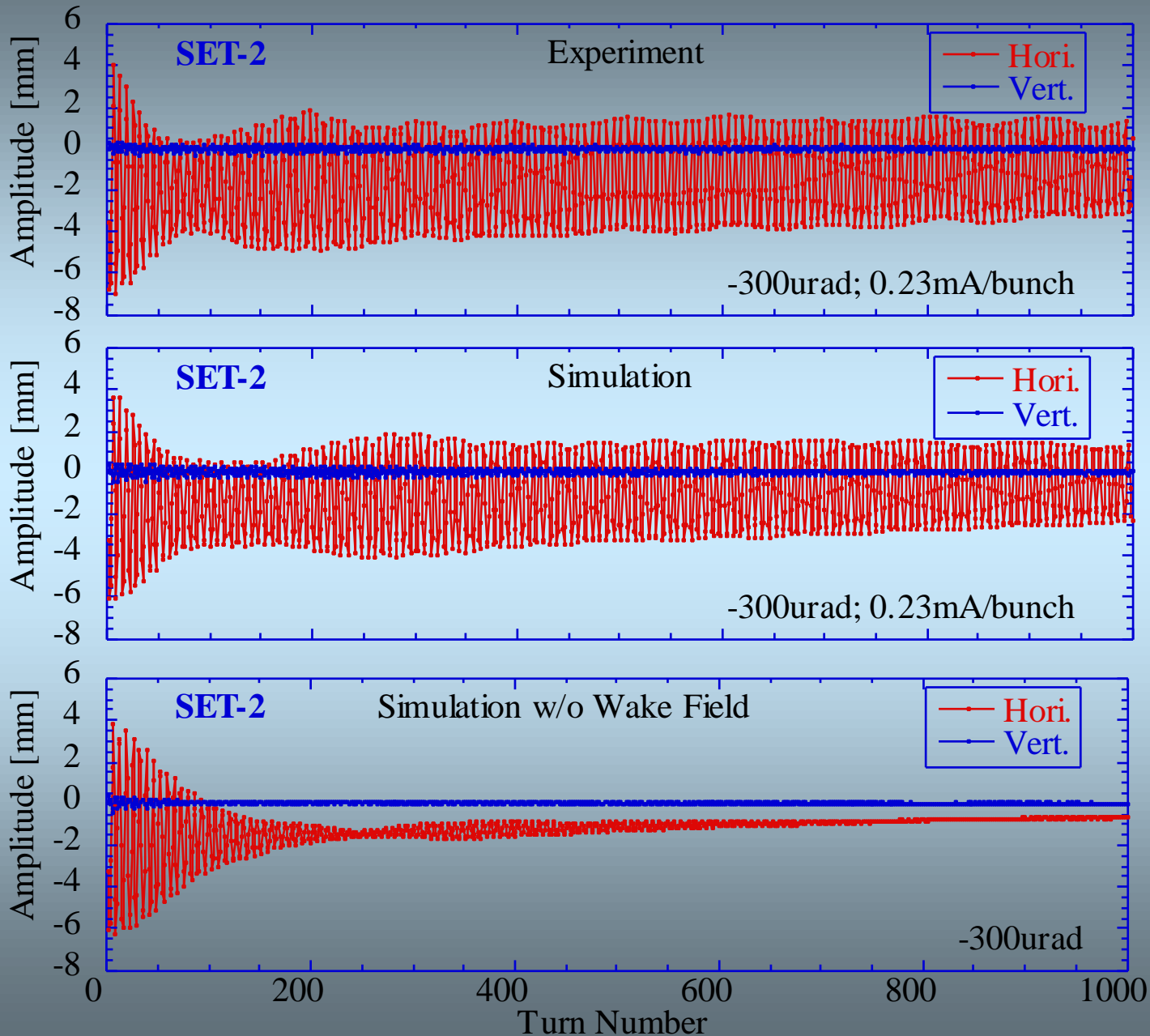
- Refs. [8] K. Halbach; NIM 187(1981)109.  
 [9] E. Forest and K. Ohmi; KEK Report 92-14 (1992).

# 3. Comparison between Simulation and Experiments

## 3.1. Amplitude Dependent Tune Shift



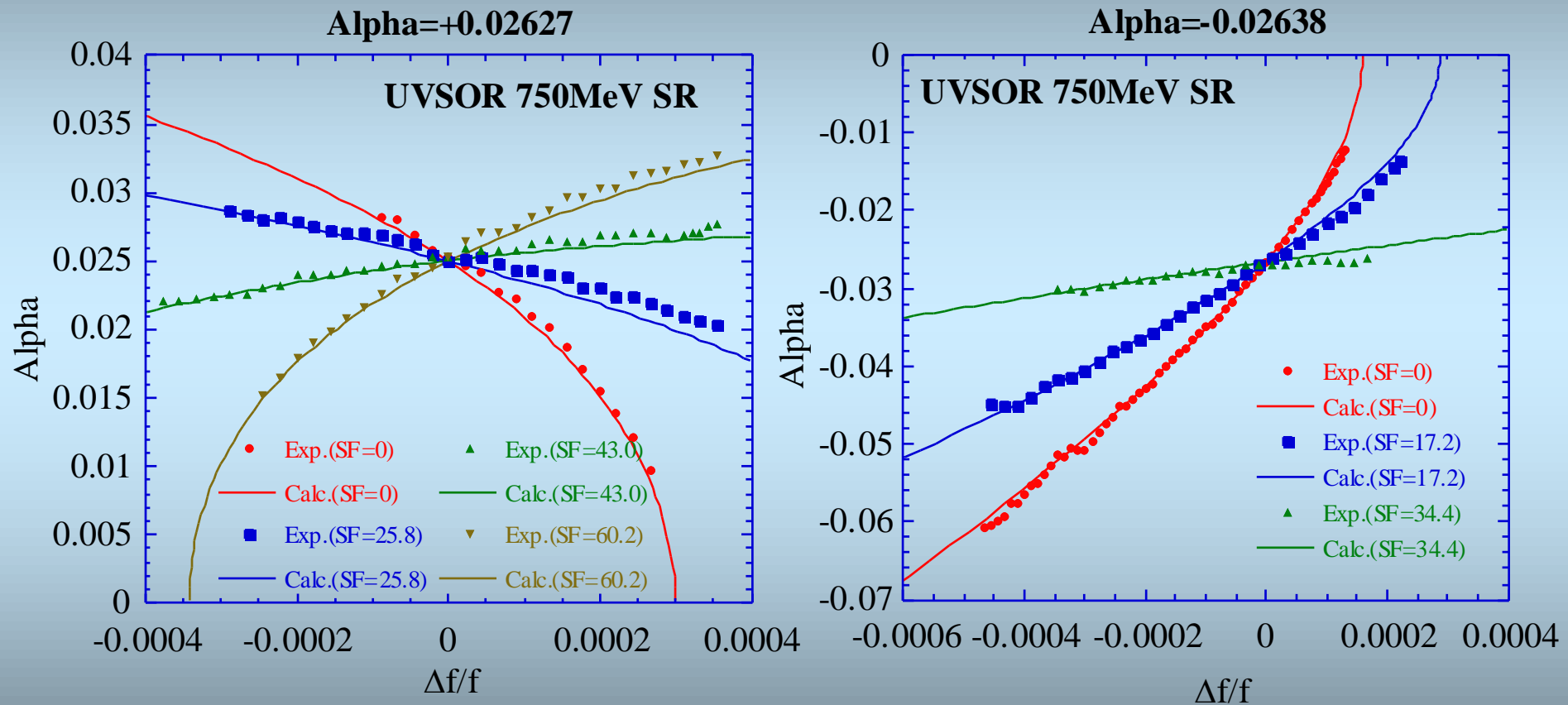
# 3.2. Smear of Coherent Oscillation



Refs. [10] K. Ohmi et.al.; PRE 59 (1999)1167.

[11] J. Schimizu et.al.; Proc. of EPAC02 (2002) p.1287.

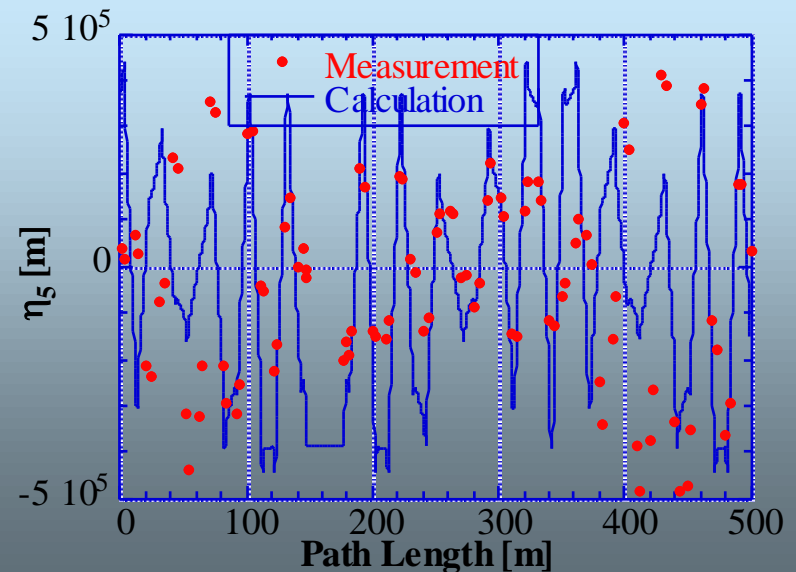
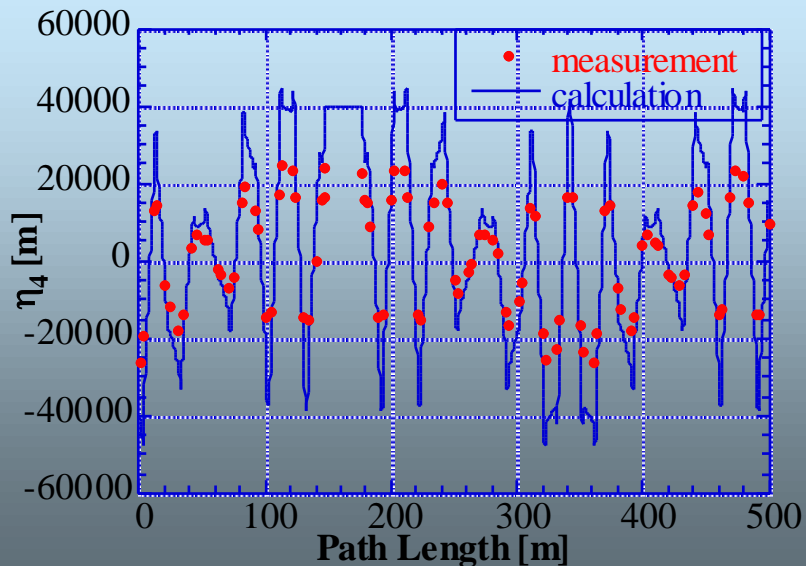
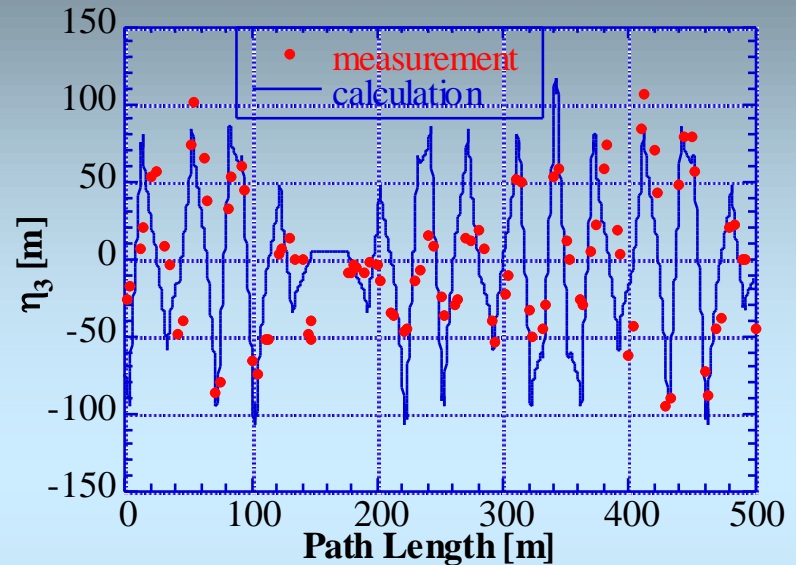
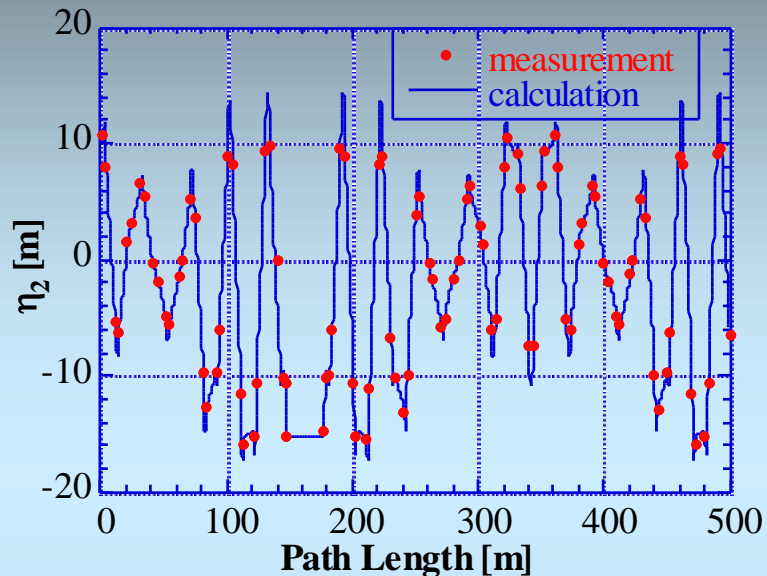
# 3.3. Nonlinear Momentum Compaction



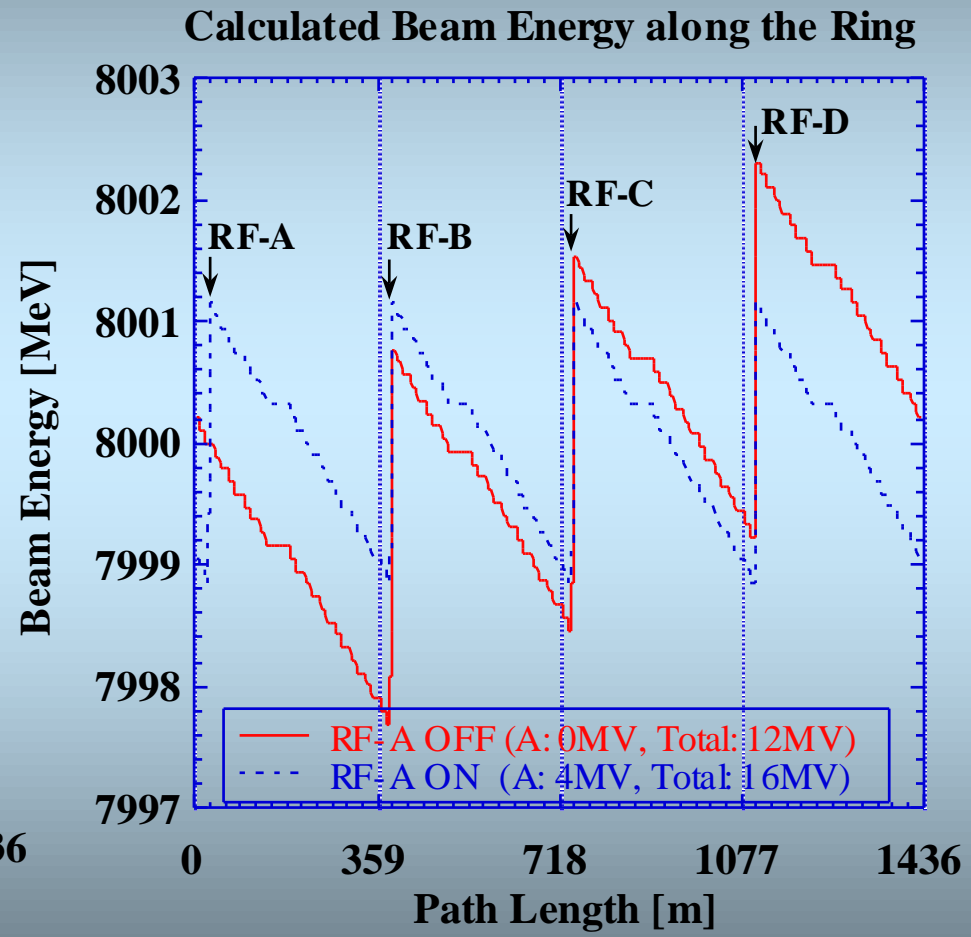
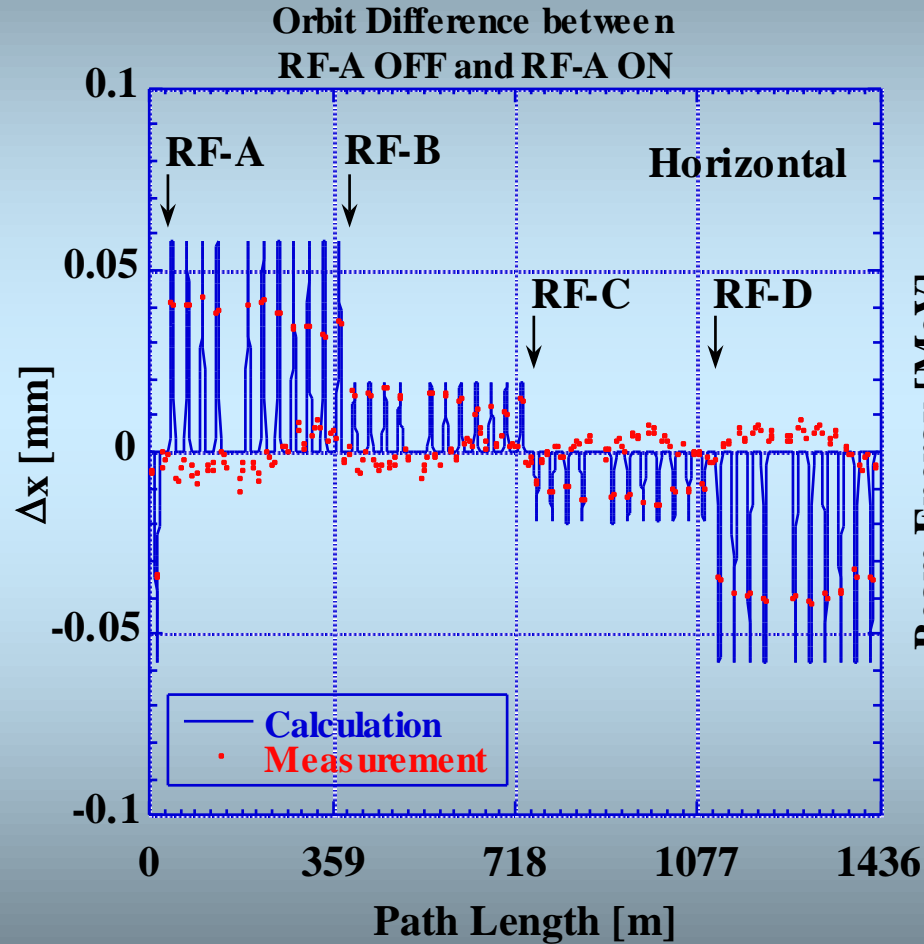
Ref. [12] H. Tanaka et.al.; NIMA 431(1999)396.

# 3.4. Nonlinear Dispersion Ref. [12]

$$\eta(\delta) = \eta_1 + \eta_2 \delta + \eta_3 \delta^2 + \eta_4 \delta^3 + \eta_5 \delta^4 \dots$$



# 3.5. 3D Closed Orbit



# 3.6. Injection Beam Loss

## 3.6.1. Parameters of Injection Beam and Injection scheme

### •Injection Beam Parameters

$\varepsilon_x=220$  nmrad,  $(\varepsilon_y/\varepsilon_x)=0.002$

$\sigma_\delta=0.0013$ ,  $\sigma_\tau=63$  psec

Optical Functions at IP

$\beta_x\sim 13.5$ m,  $\alpha_x=-0.11$

$\beta_y\sim 13.7$ m,  $\alpha_y=-0.20$

### •Injection Bump System

Injection Point:  $\Delta x=-24.5$ mm

Bump height= $\sim 14.5$ mm

Bump Pulse Width= $\sim 8$ usec

(Revolution= $\sim 4.7$ usec)

### •Aperture Limit

Septum Inner wall:  $-19.5$ mm

Chamber Aperture 70(H) / 40(V) mm

In-vacuum ID Vert. Lim.: min.7mm

### •Ring Parameters

$\varepsilon_x=2.8\sim 6.6$  nmrad, Coupling  $(\varepsilon_y/\varepsilon_x)=0.002$

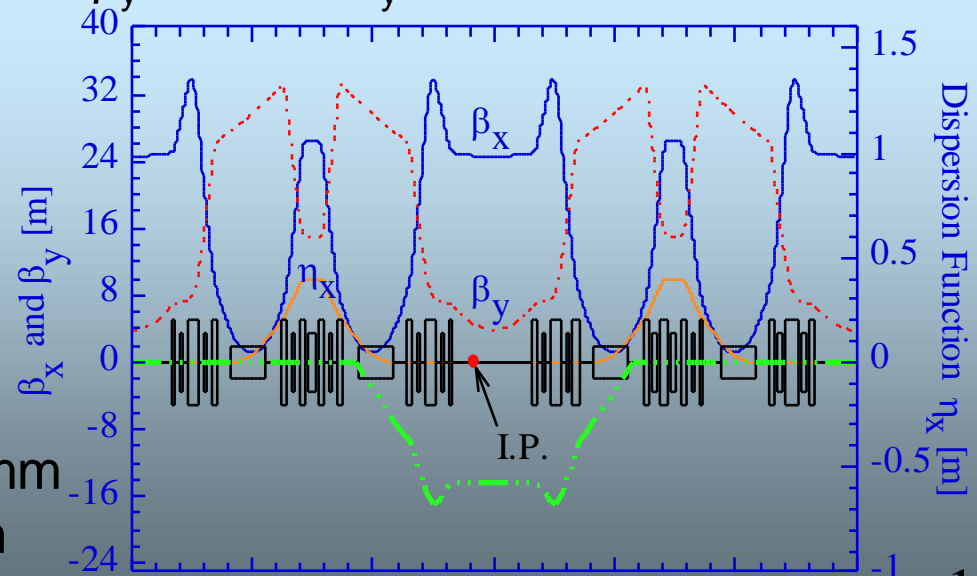
$\sigma_\delta=0.0011$ ,  $\sigma_\tau=13$  psec

$\nu_x=40.15$ ,  $\nu_y=18.35$

Optical Functions at IP

$\beta_x\sim 23$ m,  $\alpha_x=-0.2$

$\beta_y\sim 7.5$ m,  $\alpha_y=-0.45$





## 3.6.2. ID Parameters(1)

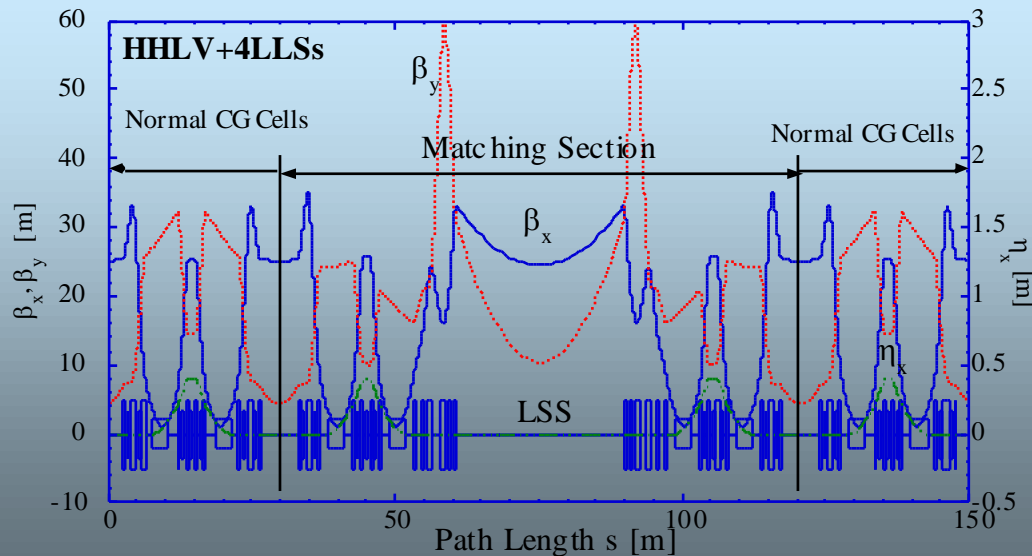
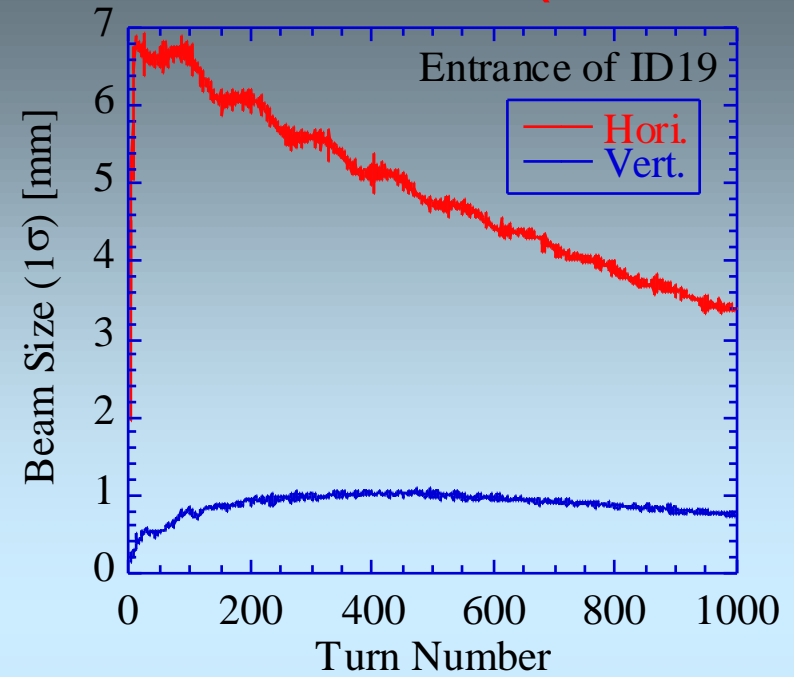
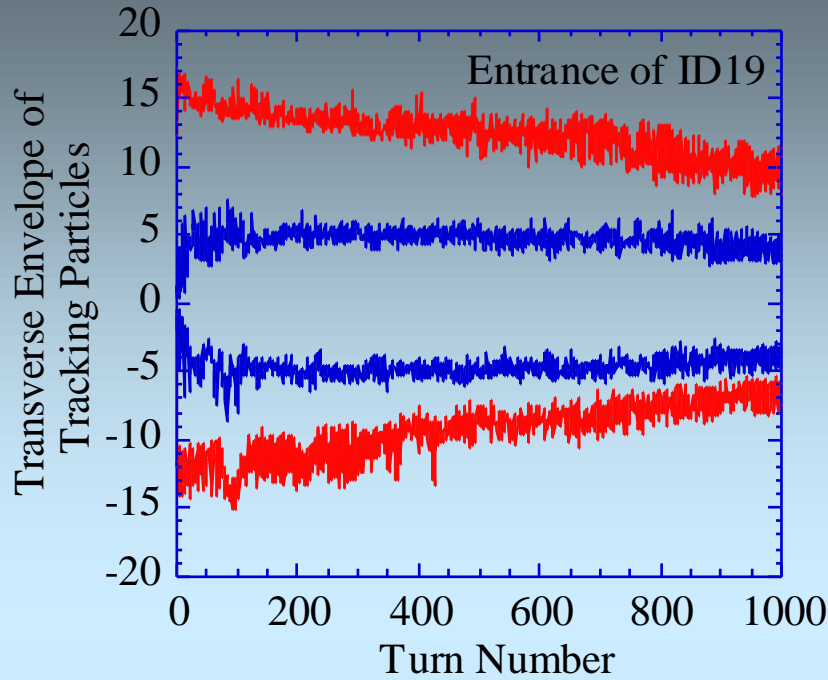
#	Min.Gap [mm]	Kx	Ky	Power [kW]	Type
19	12		1.8	35	<b>In-Vacuum Long</b>
20	7		2.1	14	In-Vacuum Hybrid
9	9.6		2.1	8.8	In-Vacuum Standard
10	9.6		2.2	9.6	In-Vacuum Standard
11	9.6		2.2	9.9	In-Vacuum Standard
12	9.6		2.2	9.6	In-Vacuum Standard
13	9.6		2.2	9.8	In-Vacuum Standard
16	12.9		2.4	7.4	In-Vacuum
22	9.98		2.9	12.3	In-Vacuum
24	9.6	1.3	1.4	4	<b>In-Vacuum Figure-8</b>
29	8.8		2.4	11.2	In-Vacuum Standard
35	9		2.3	10.8	In-Vacuum Standard
37	8		2.6	13.3	In-Vacuum Standard
39	8.6		2.3	10.9	In-Vacuum Standard
40	8.3	1.1	1.0	3.5	<b>In-Vacuum Helical</b>
41	9.6		2.0	8.1	In-Vacuum Standard
44	9		2.3	10.9	In-Vacuum Standard
45	8	1.7		1.4	<b>In-Vacuum Vertical tandem</b>
46	8		1.5	8.1	In-Vacuum Hybrid
47	9.6		2.1	9.1	In-Vacuum Standard

## 3.6.2. ID Parameters(2)

#	Min.Gap [mm]	Kx	Ky	Power [kW]	Type
8	25.5	1.1	11.2	18.04	Out-Vacuum Elliptical Wiggler
15	20.0		2.2	5.4	Out-Vacuum Revolver (Linear)
	20.0	3.4	3.4	5.6	Out-Vacuum Revolver (Helical)
25	30.0	4.8	4.6	2	Out-Vacuum Helical tandem
27	37.0	3.9	5.4	6.6	Out-Vacuum Figure-8
23	36.0	3.4	3.4		Out-Vacuum APPLE-II (Circular)
	36.0		5.8		Out-Vacuum APPLE-II (Linear)
	36.0	4.2			Out-Vacuum APPLE-II (Vertical)
17*	20.0				Installed but under commissioning

\* ID 17 was recently installed in the ring. Gap of ID 17 is usually closed. The phase is shifted so that the magnetic field is cancelled out at the center. The field is no zero and nonlinear at the off-center.

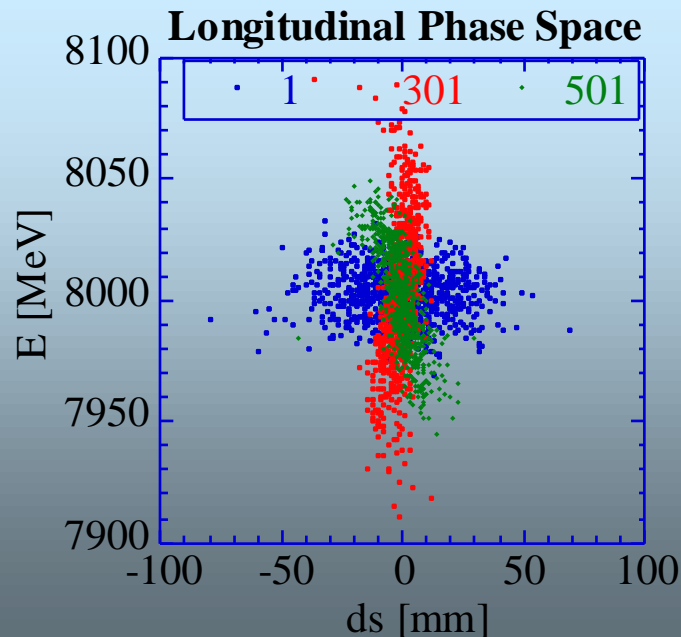
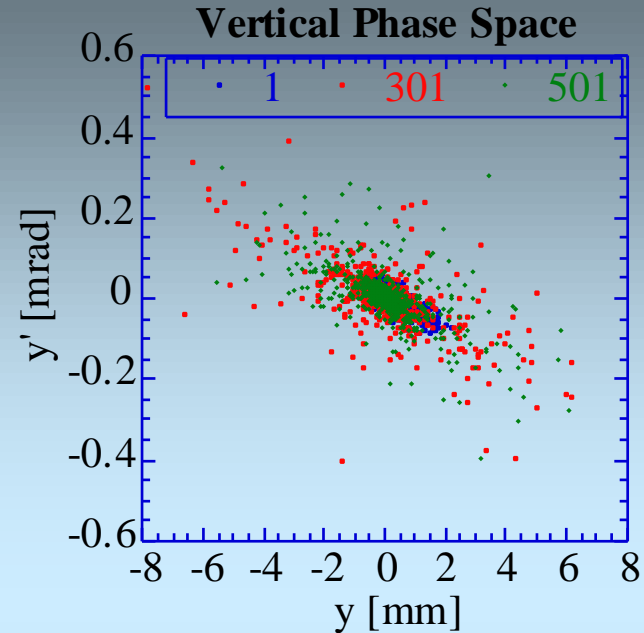
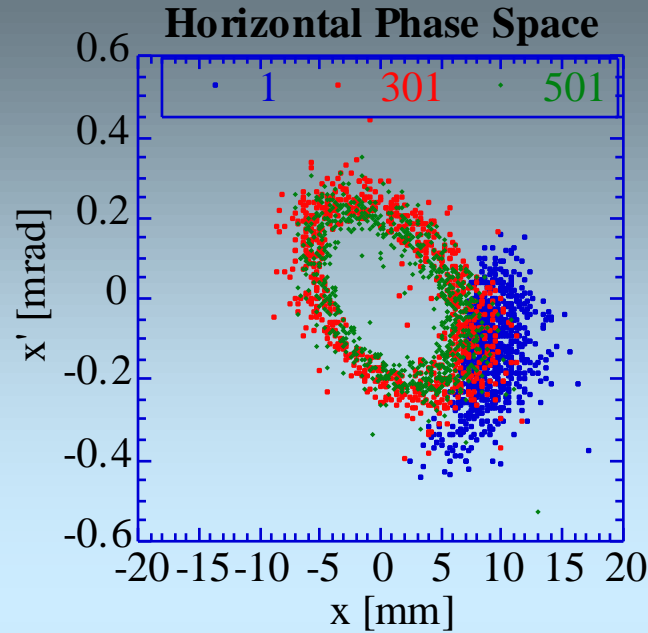
# 3.6.3. Behaviour of Injection Beam (1-Calc)



In simulation, particles are mainly lost :

- Septum wall (Hori.)
- LSS beta-peak (Vert.)
- IDs (Vert.)

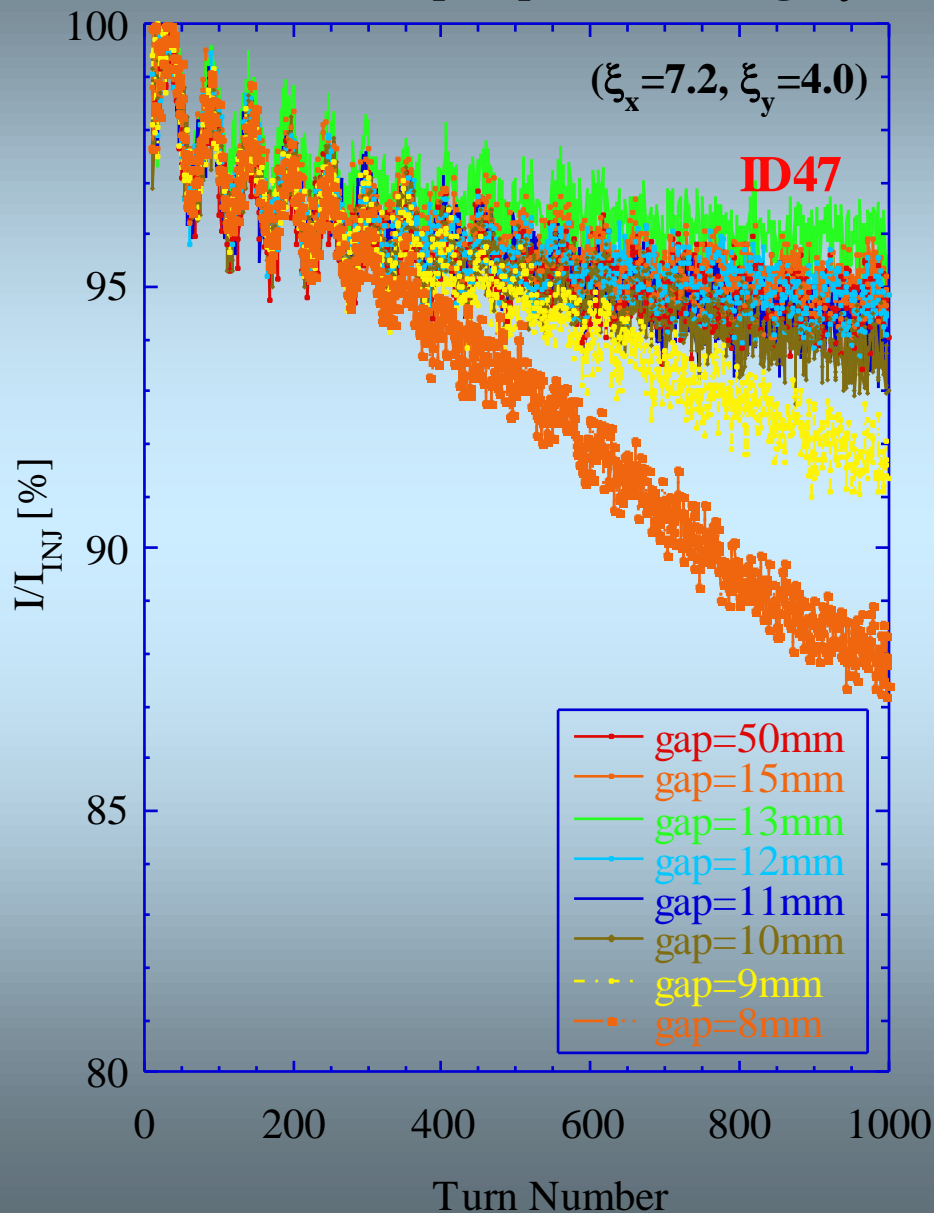
# 3.6.3. Behaviour of Injection Beam (2-Calc)



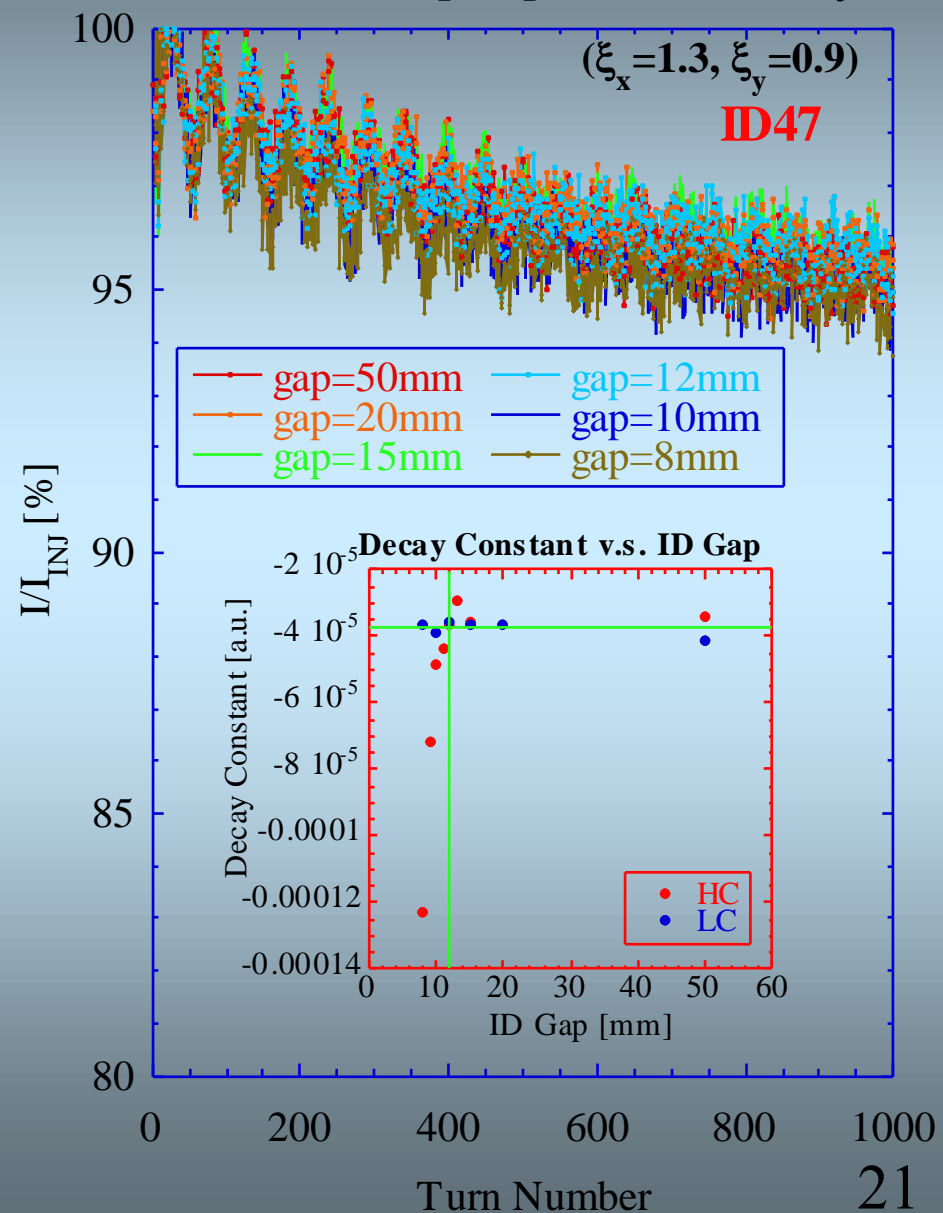
Observation Point:  
Entrance of ID19

# 3.6.4. Beam Loss v.s. Gap of ID47(1)

Measured Gap Dependence@High  $\xi$

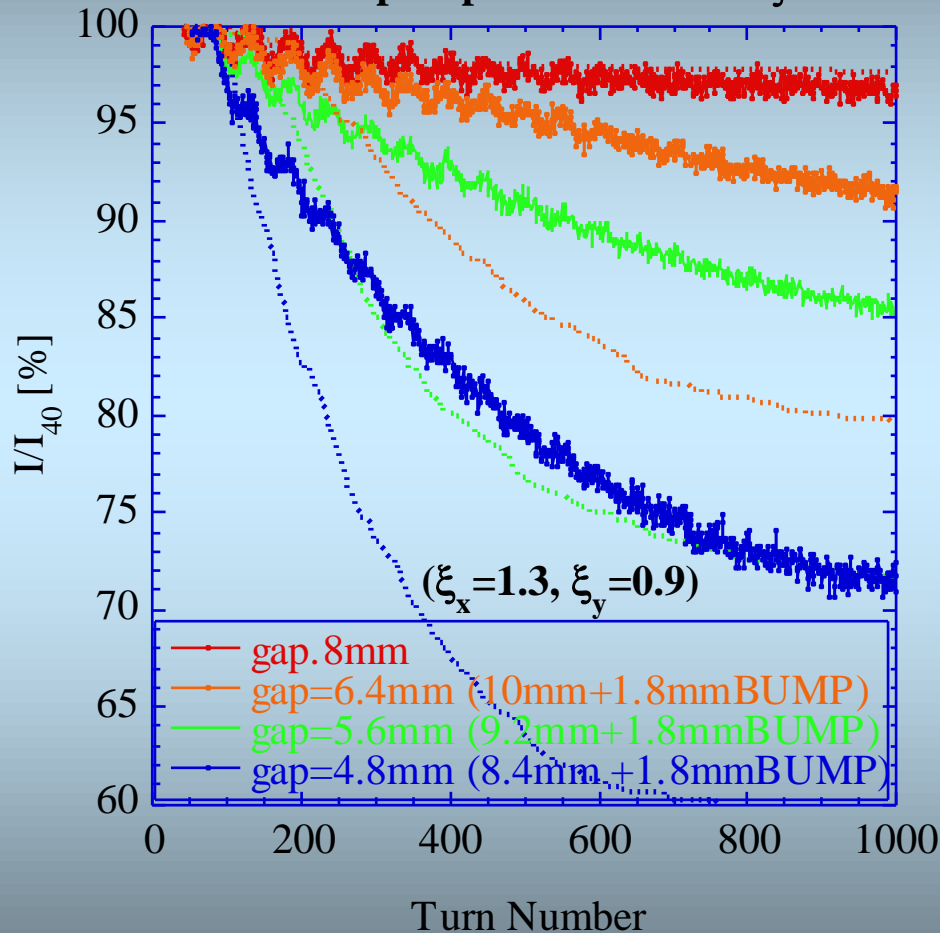


Measured Gap Dependence@Low  $\xi$

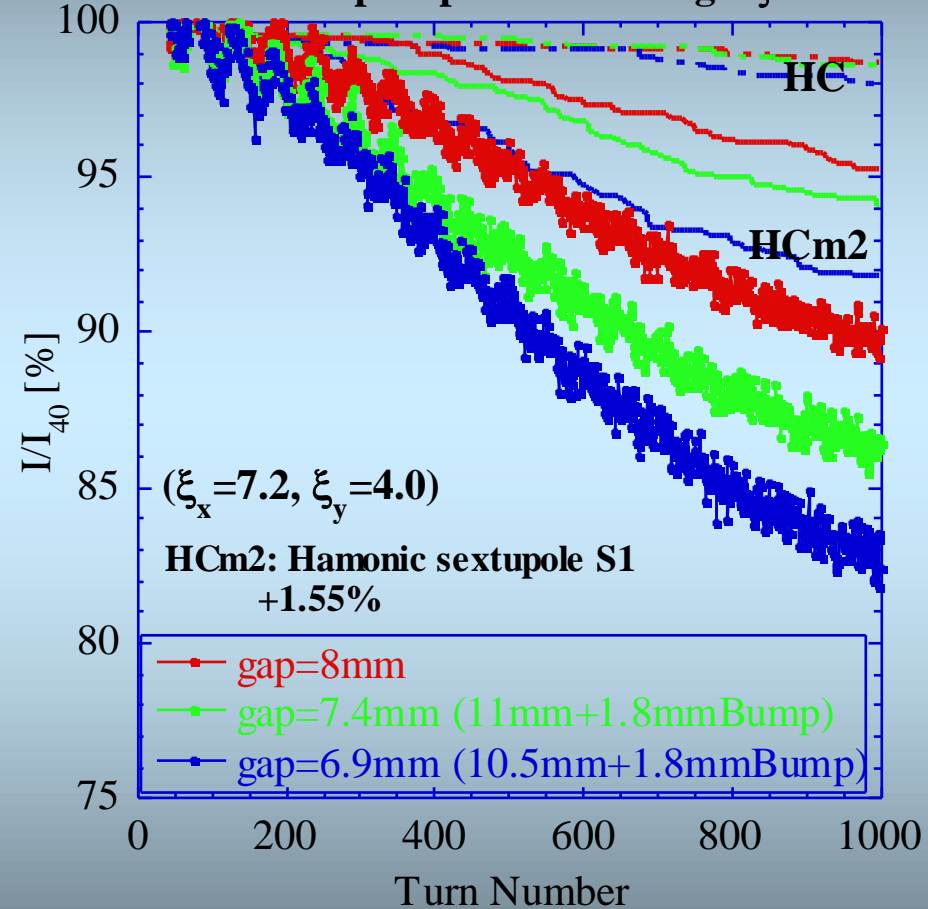


# 3.6.4. Beam Loss v.s. Gap of ID47(2)

ID Gap Dependence@Low  $\xi$

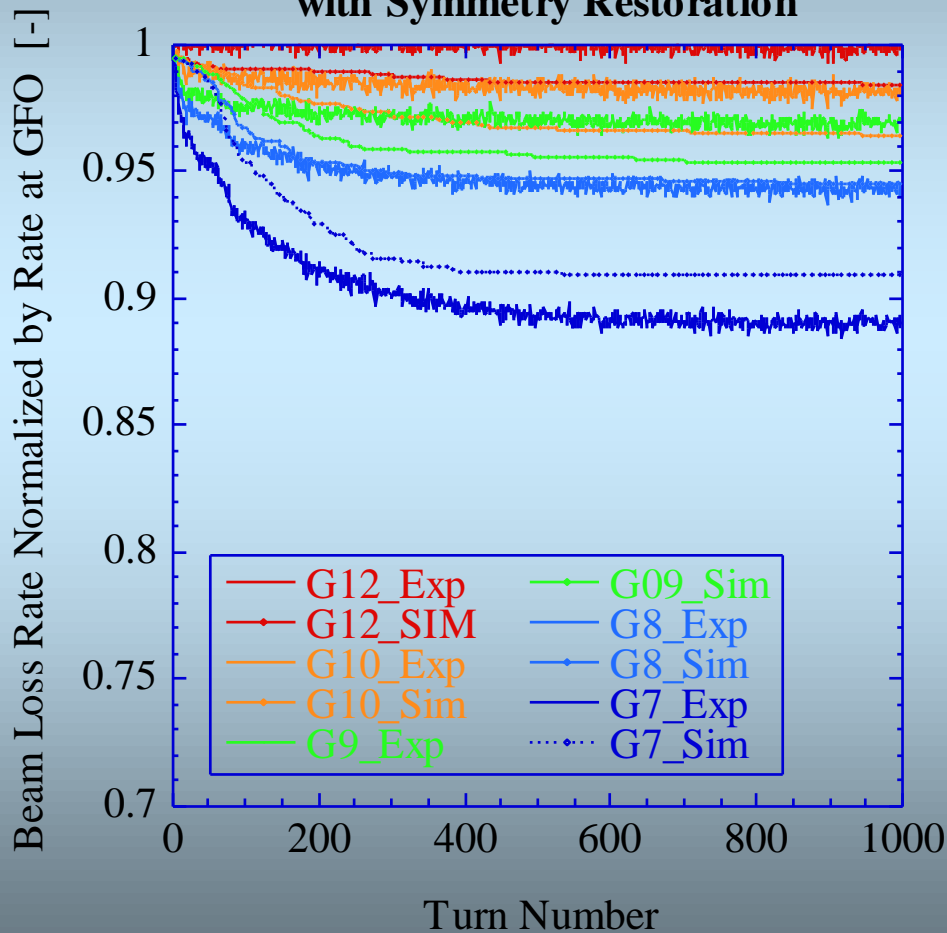


ID Gap Dependence@High  $\xi$

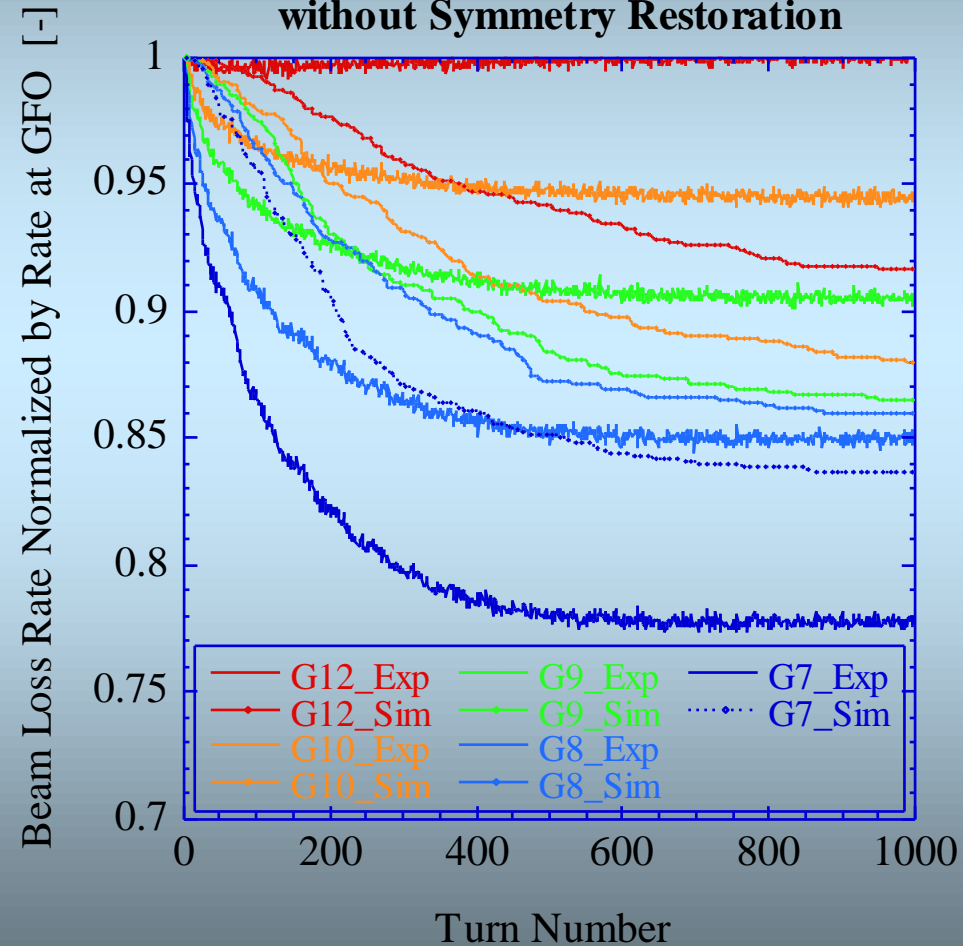


# 3.6.5. Beam Loss v.s. Symmetry restoration of Optics

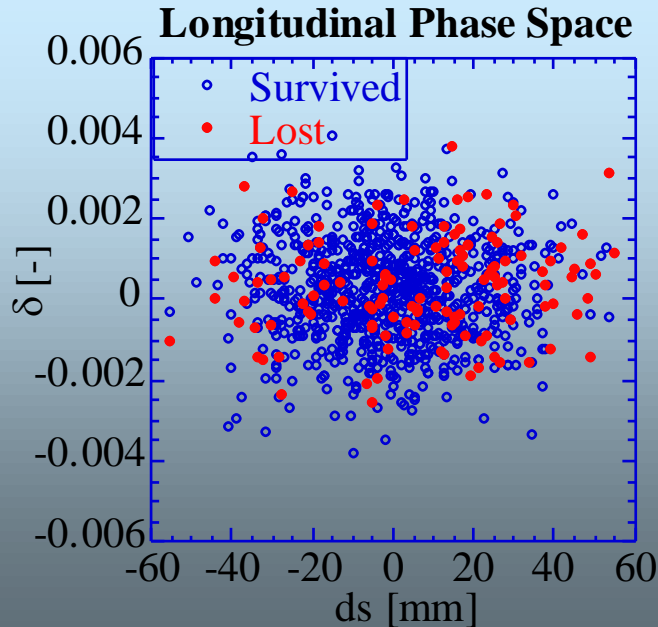
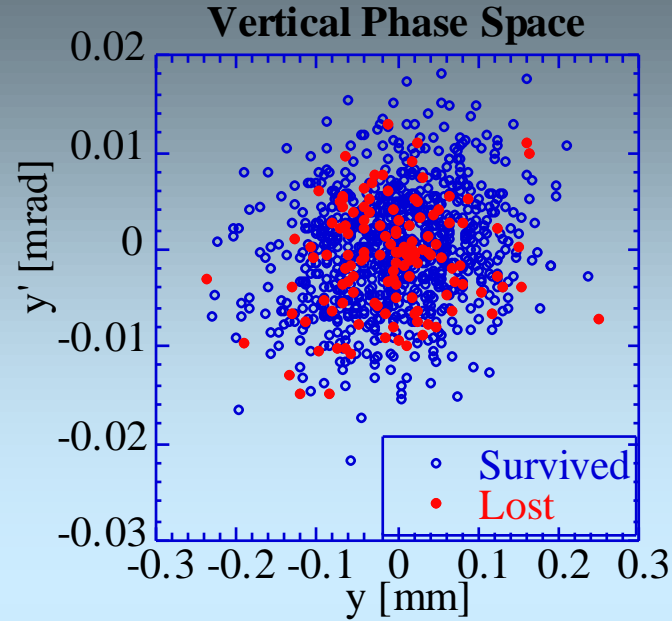
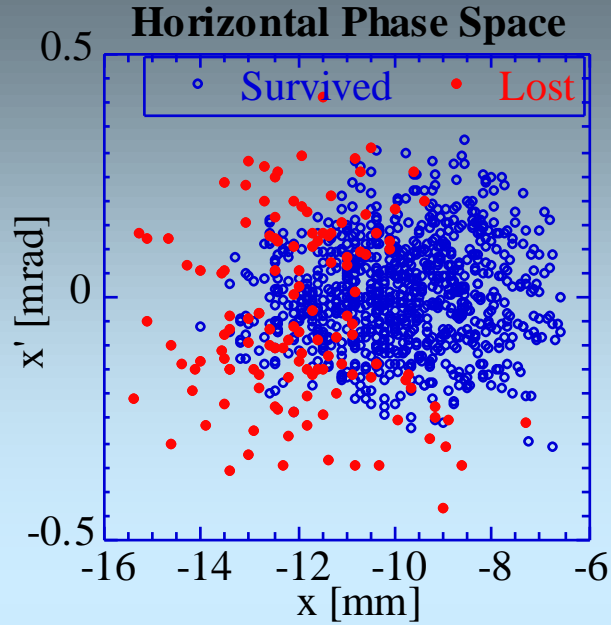
Gap Dependence of Loss Rate @ID20 with Symmetry Restoration



Gap Dependence of Loss Rate @ID20 without Symmetry Restoration



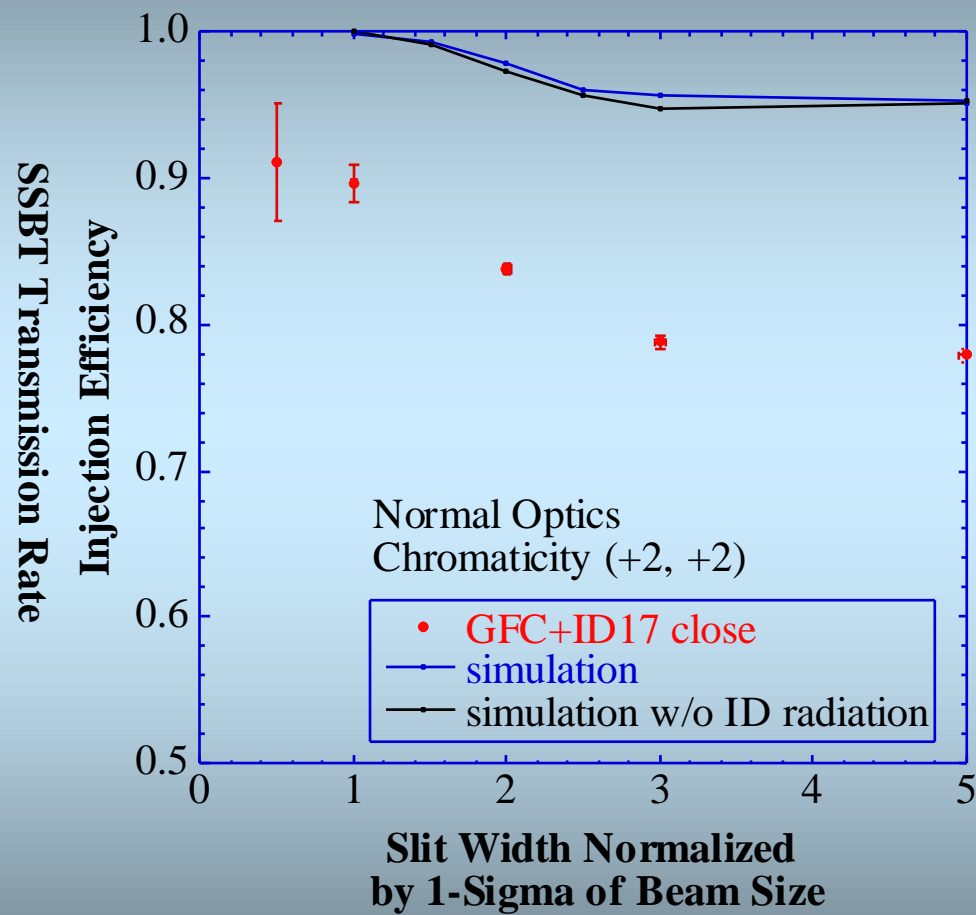
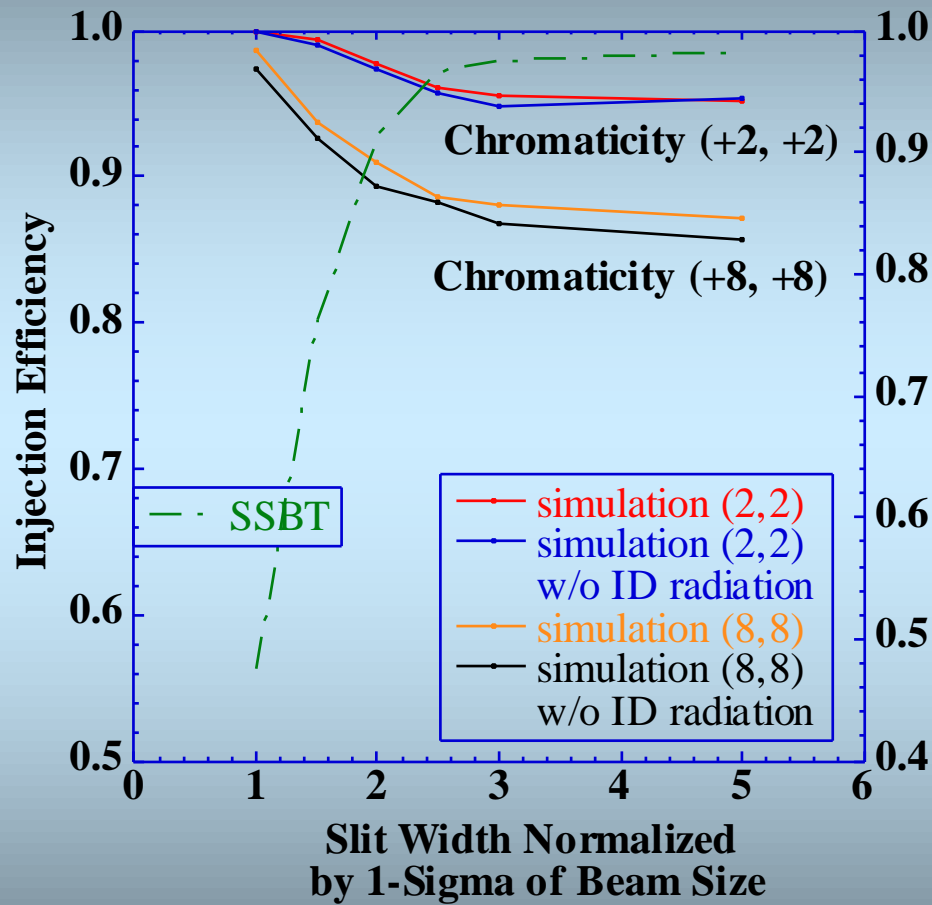
# 3.6.6. Beam Loss v.s. Initial Condition (Calc)



Lost particles have clear correlation with horizontal emittance .



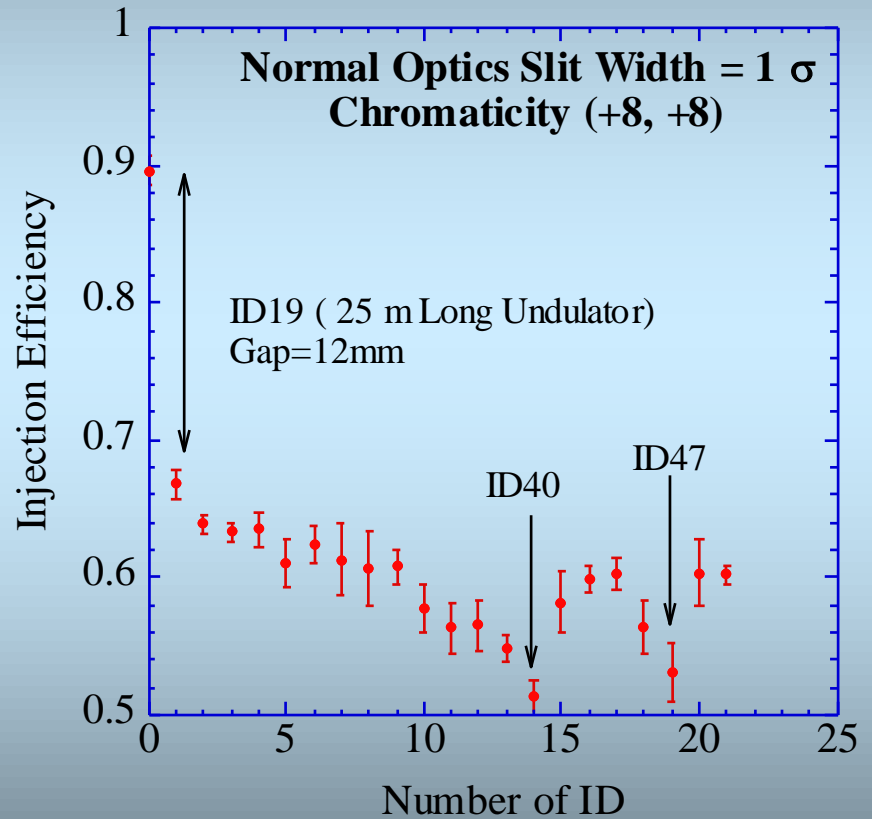
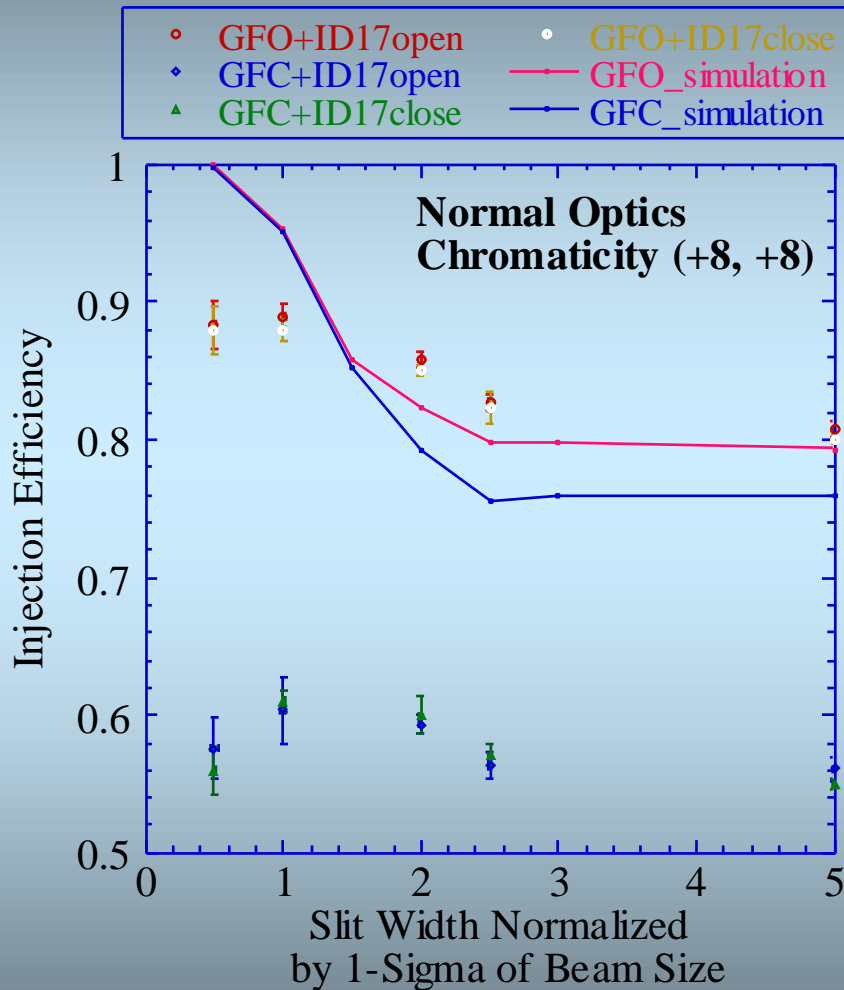
# 3.6.7. Beam Loss v.s. Beam Collimation (1)



Planner type IDs are only considered in the simulation.

# 3.6.7. Beam Loss v.s. Beam Collimation (2)

**Injection orbit is shifted to septum wall by 2mm**



Planner type IDs are only considered in the simulation.

# 4. Summary(1)

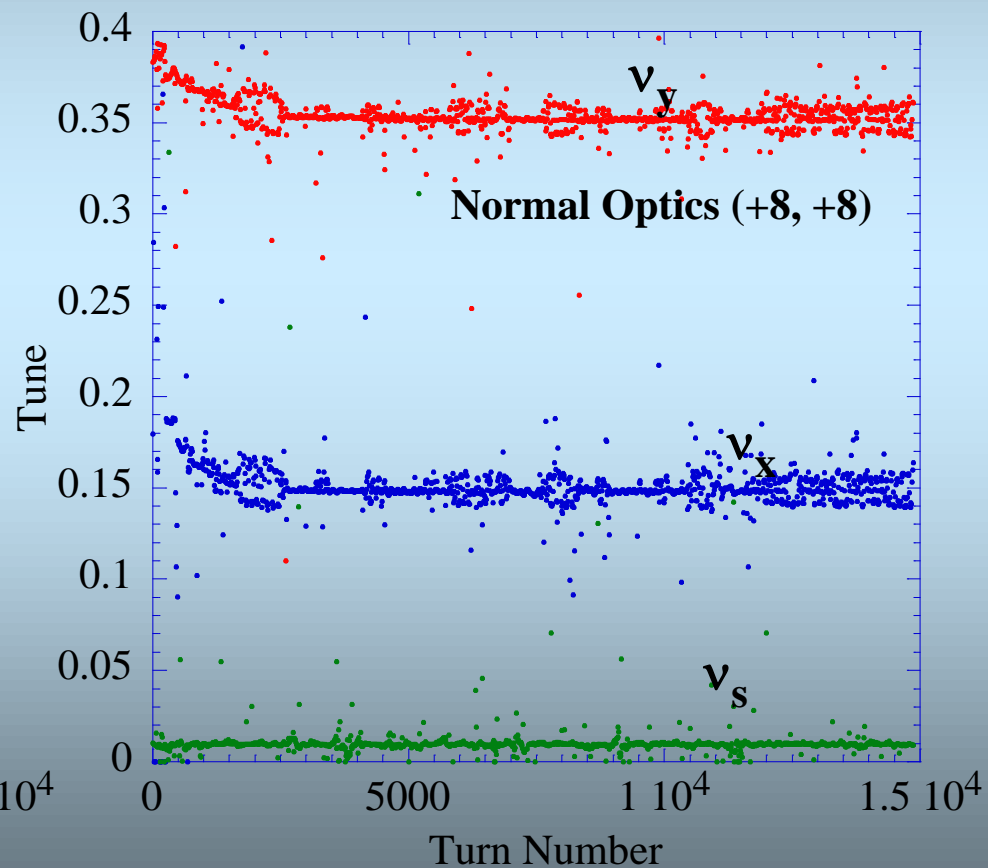
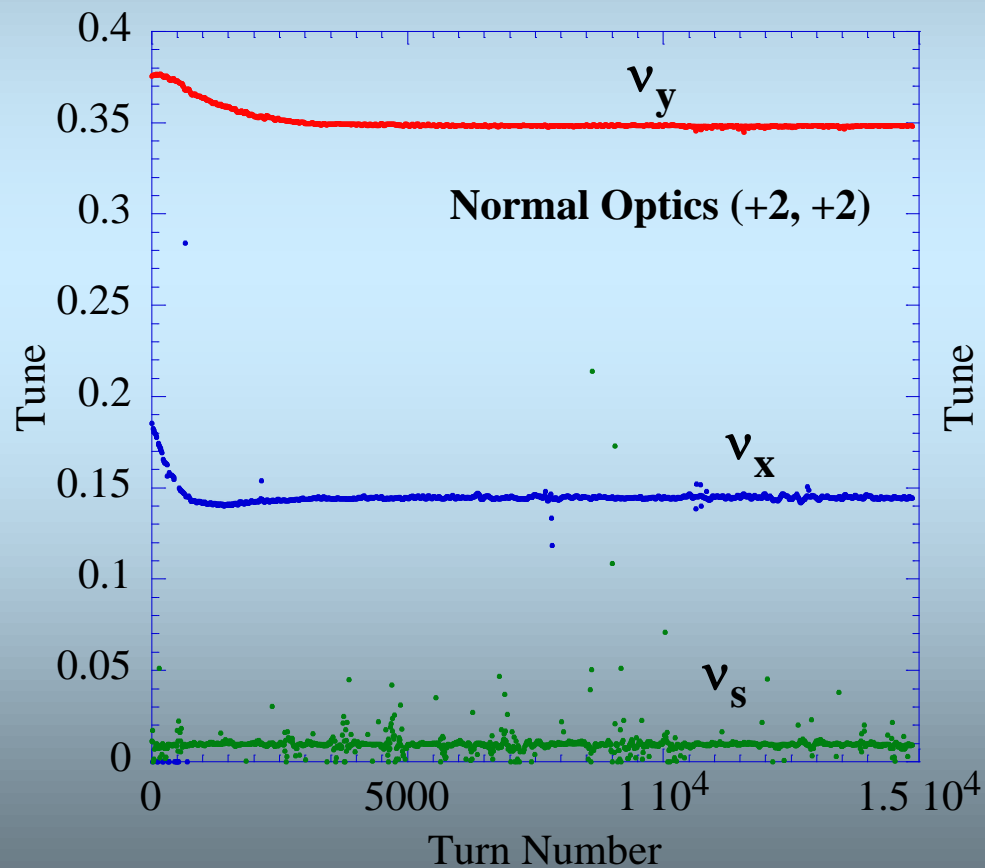
- Developed simulator well describes nonlinear particle motion in a storage ring. However, the simulator can not explain injection beam loss quantitatively.
- Possible causes are:
  - Ambiguity in injection beam distribution
  - Incorrect ID Modeling at especially large amplitude
  - Nonlinearity not included in the model
  - Some mistake in calculation, etc

## 4. Summary(2)

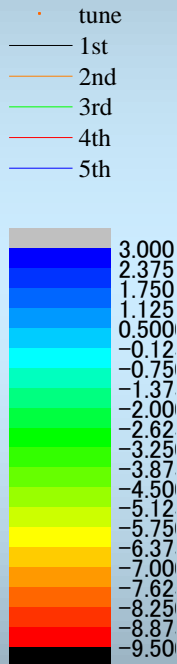
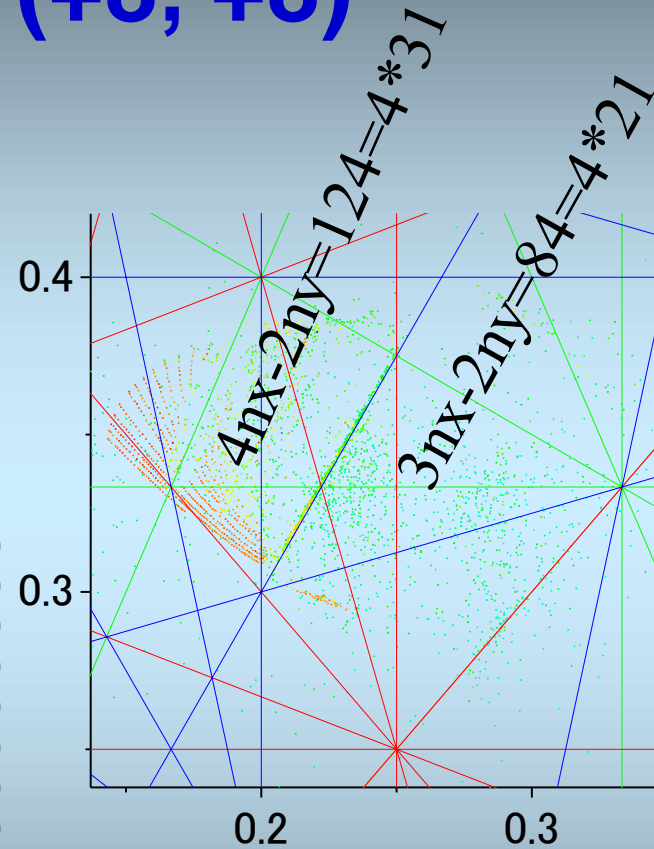
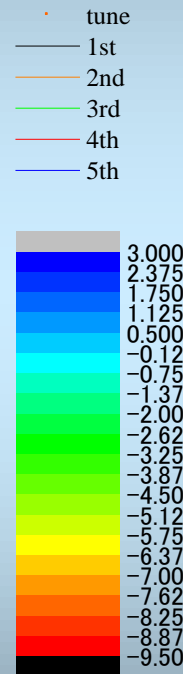
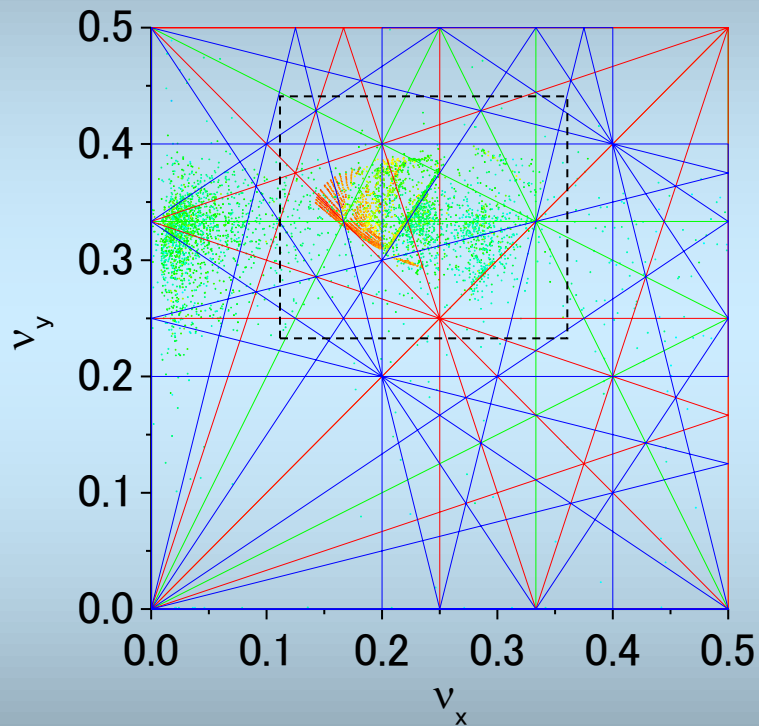
- Frequency Map Analysis (FMA) could be a powerful tool to investigate mechanism of injection beam loss.
- To use FMA effectively, we need “ a precise ring model”.

# 5. Tentative FMA Results

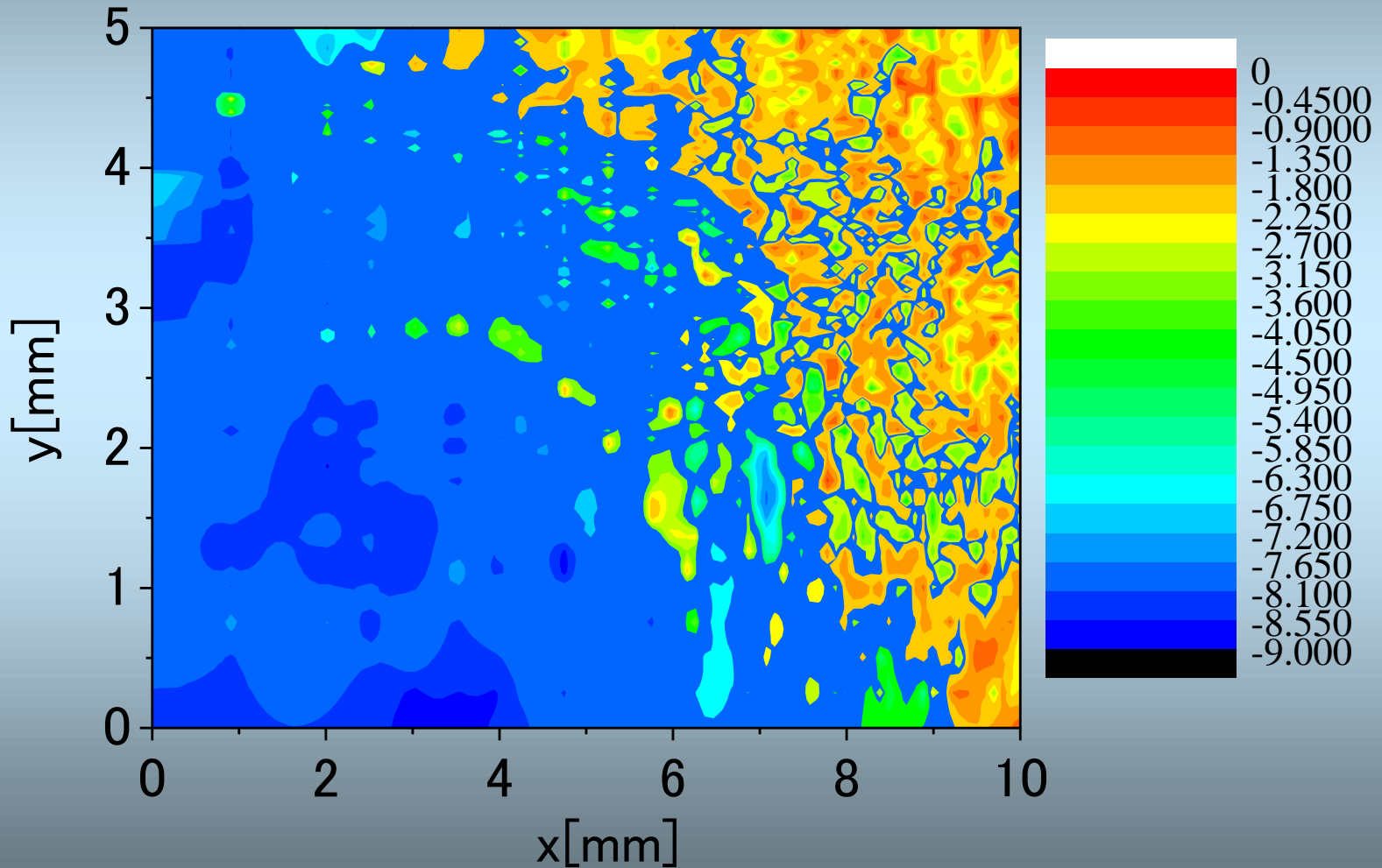
Tune modulation in damping of injection beam



# FMA of Normal Optics w/o Errors Chromaticity (+8, +8)

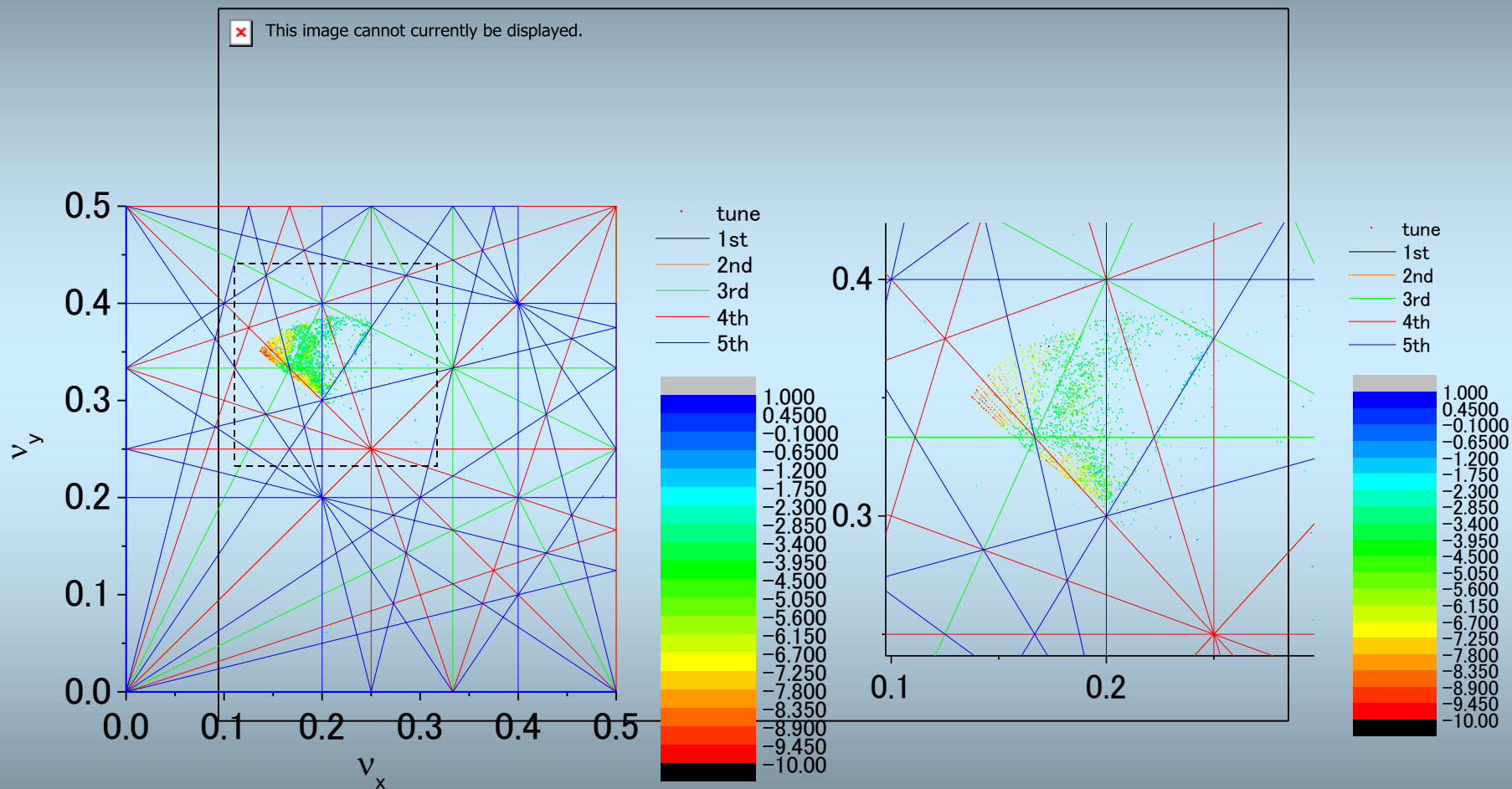


# Stability Map of Normal Optics w/o Errors Chromaticity (+8, +8)



# FMA of Normal Optics with Errors

## Chromaticity (+8, +8)





# Stability Map of Normal Optics with Errors Chromaticity (+8, +8)

